Bull. Mater. Sci., Vol. 9, No. 3, August 1987, pp. 169–180. © Printed in India.

Dielectric behaviour of ZnO-based ceramic semiconductors

SUBHASH C KASHYAP†, K L CHOPRA* and BHARAT BHUSHAN**

Centre for Materials Science and Technology, Indian Institute of Technology, New Delhi 110 016, India

*Indian Institute of Technology, Kharagpur 721 302, India

**Present address: Semiconductor Complex Ltd., Chandigarh, India

MS received 9 June 1987

Abstract. The effect of composition, sintering parameters, frequency and temperature on the dielectric parameters of ZnO-based ceramic semiconductors (cersems) having small amounts of Bi_2O_3, Sb_2O_3, CoO, MnO_2, La_2O_3 and/or Cr_2O_3 has been investigated. The unusually high dielectric constant of these composites, arising due to a two-phase microstructure has been explained on the basis of a depletion layer model. The agreement in values of barrier height and donor concentration calculated from $C^{-2}-V$ plot, Hall measurement and I-V characteristics of these cersems supports the validity of barrier and depletion layer models. The depletion and inter-granular layers are estimated to be nearly 10^2 nm and 1–2 nm respectively. The observed variation of dielectric constant/capacitance with sintering parameters and temperature of measurement has also been explained on the basis of simplified microstructure and depletion layers. The loss peak (f_{max}) observed at 300 kHz remains practically unaltered with change in composition and sintering parameters. The observed dielectric dispersion in the range 10^2–10^6 Hz, exhibiting multiple relaxation times and activation energy of relaxation process as 0·36 eV, has been explained on the basis of Debye-type relaxation process originating due to trapping/detrapping and possibly due to scattering of carriers in the depletion regions.

Keywords. Dielectrics; ceramic semiconductors; zinc oxide; relaxation phenomena; varistors.

1. Introduction

Zinc oxide-based ceramic semiconductors (cersems), prepared by sintering of ZnO with one or more of the oxide additives like Bi_2O_3, BaO, Sb_2O_3, CoO, MnO_2 and/or Cr_2O_3 are known to exhibit a remarkable nonlinear current (I)-voltage (V) characteristics given by $I = KV^{\alpha}$, where the exponent α having a typical value of 50 is a measure of nonlinearity (Matsuoka 1971; Levinson and Philipp 1975; Mukae *et al* 1977; Bhushan *et al* 1981; Eda *et al* 1983). Microstructurally a ZnO nonlinear cersem is a two-phase composite having semiconducting/conducting ZnO grains embedded in thin insulating intergranular layers of additives of varying thickness estimated to lie between 10 nm and 1 μm (Matsuoka 1971; Levinson and Philipp 1975, 1976; Morris 1976; Clarke 1978; Santhanam *et al* 1979). Owing to their large current-carrying capacity and quick response time these composites find tremendous application potential as varistors.

There are only a few reports which exclusively discuss the dielectric properties of ZnO cersems (Delaney and Kaiser 1967; Levinson and Philipp 1976, 1978; Matsuura and Yamaoki 1977; Chopra *et al* 1983). In some other cases only a mention of

†To whom all correspondence should be addressed.

strikingly high dielectric constant and/or appearance of loss peak at or nearly at 300 kHz has been made (Eda *et al* 1980; Bhushan *et al* 1981). The observed broad peak in dielectric loss ($\tan\delta$) vs frequency curve could not be attributed to any single model. Whereas Levinson and Philipp (1976, 1978) rejected the Maxwell-Wagner model of interfacial polarization at temperatures other than 4 K, and explained the observed dispersion on the basis of defect-states model. Matsuura and Yamaoki (1977) simulated the Maxwell-Wagner model to fit the observed loss curves of ZnO varistors. In some cases the estimated high value of dielectric constant (~ 1000) and the capacitance value of 0·18 μF/cm^2/grain have been ascribed to the insulating inter-granular layers (Matsuoka 1971; Levinson and Philipp 1975; Morris 1976).

In order to understand the role of microstructure, composition and inter-granular potential barrier on the observed dielectric properties of ZnO-based cersems, these composites have been systematically investigated in the present study. Results of the effect of composition and sintering parameters on the dielectric properties and dependence of dielectric parameters on frequency, temperature and bias voltage are discussed.

2. Experimental

Zinc oxide cersems having different combinations of additives were prepared by a standard ceramic sintering technique. Mechanically polished and ultrasonically cleaned samples were annealed at 200°C in a vacuum of about 10^{-5} torr for 30 min so that any adsorbed gases or volatile impurities are removed. Dielectric constant (ε') and dielectric loss ($\tan\delta$) of the composites were measured at different temperatures ranging from 200 to 400 K in the frequency range of 10^2 to 10^6 Hz by employing an LCR bridge and a Wayne-Kerr bridge. That the measurements are not affected by the electrode capacitance is confirmed by the observation that the dielectric parameters thus measured are independent of sample thickness. Bias dependence of capacitance was plotted at a fixed frequency of 10^6 Hz using a C-V plotter (Plotomatic 715 MSI Electronics).

The composition (elemental) analysis and depth profile of various cersems were obtained by Auger electron spectroscopy technique using a super SAM 590A instrument. An electron beam of 0·2 μ diameter with 0–10 kV energy was used in scanning mode. Analysis could be done in both the spot as well as scanning mode, with a spatial resolution of about 0·2 μ. The depth profile of various constituent elements was achieved by etching with a calibrated 5 kV argon ion beam of 300 μ diameter which could be rastered over different areas ranging from 1×1 mm^2 to 10×10 mm^2.

3. Results and discussion

3.1 *High dielectric constant and depletion layer model*

The values of capacitance and dielectric constant of various cersems having different compositions and prepared under varied experimental conditions are presented in table 1. It can be seen that the composites showing linear I-V characteristics exhibit

Table 1. Capacitance/dielectric constant of various ZnO cersems measured at 10^3 Hz.

Sample	Sintering temperature (°C)	Capacitance/cm² (sample thickness = 1 mm) (pF/cm²)	Capacitance (μF/cm²/G.B.)	Dielectric constant
$ZnO\text{-}Cr_2O_3$	1200	24	—	26^L
ZnO-CoO	1200	20	—	22^L
$ZnO\text{-}Bi_2O_3$,M	800	17	—	19^L
$ZnO\text{-}Bi_2O_3$,M	900	570	0·20	450^N
$ZnO\text{-}Bi_2O_3$,M	1000	1000	0·22	820^N
$ZnO\text{-}Bi_2O_3$,M	1200	2600	0·27	2080^N
$ZnO\text{-}CoO\text{-}La_2O_3$	1200	3700	0·26	2960^N

L, linear (ohmic) system; N, nonlinear (nonohmic) system; M, multicomponent.

values of dielectric constant (ε') which are comparable to those for the constituent oxides ($\varepsilon' = 10$ to 30), whereas all the cersems exhibiting nonlinear characteristics have shown higher values ($\sim 10^3$) of dielectric constant. A typical multicomponent composite of ZnO, having 0·5 mol% of each of the additives including Bi_2O_3, MnO_2, CoO and Sb_2O_3, hereafter referred to as $ZnO\text{-}Bi_2O_3$, M, sintered at 1200°C has a dielectric constant of 2080 whereas its constituents have values of dielectric constant below 30.

It may be noted that the nonlinear behaviour in cersems is caused by a two-phase microstructure and that only nonlinear cersems have a strikingly high value of dielectric constant. This implies that a two-phase microstructure is a pre-requisite for observing abnormally high values of dielectric constant. In order to quantitatively account for the observed value of dielectric constant/capacitance, the two-phase microstructure can be idealized as depicted in figure 1a and further simplified, as in figure 1b, by neglecting the contribution of interfaces which are perpendicular to

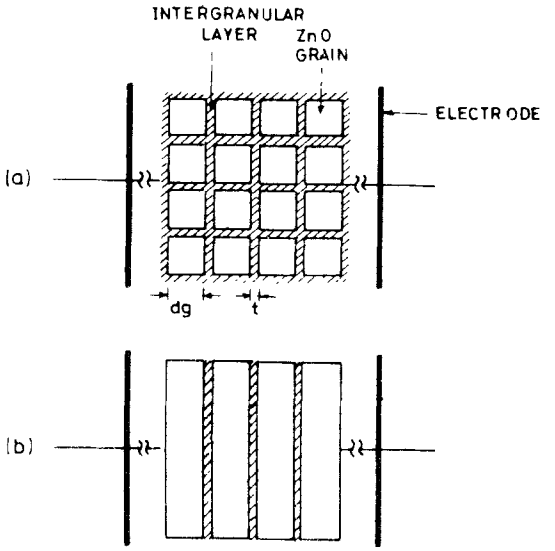

Figure 1. Sketch of an equivalent microstructure of a ZnO multicomponent nonlinear cersem.

electrodes. The total cross-section of the grains in each column, parallel to an electrode, is approximated to the area of the electrode itself, for nearly 1 nm thick intergranular layer can be neglected in comparison to the grain size of 10 μm.

A sequential mild etching with extremely low rates (1 nm/min) followed by an Auger scan was performed to carry out the depth profile. Etching was preferred over ion-induced depth-profiling due to charging of the specimen by ion-beam and extreme thinness of the intergranular layer in question. Typical Auger scans on both the unetched and etched surfaces are shown in figure 2. It is interesting to note that the carbon signal appearing due to contamination of the sample surface and Bi signal ($N_6O_{4,5}O_{4,5}$: 101 eV) vanish and the Zn signal ($M_1M_{4,5}M_{4,5}$: 107 eV) enhances after ion etching. This implies that ZnO grains are initially coated with a Bi_2O_3-rich layer and the thickness of the intergranular layers is nearly 1 to 2 nm.

Using the expression for the capacitance of a cersem in the simplified geometry of figure 1b, the value of $C/\text{area} = \varepsilon_0\varepsilon'/nt$, (where ε' is the dielectric constant of additives (~ 20), t, the thickness of intergranular layer and n, the number of intergranular layers per mm) comes out to be about 10^5 PF/cm^2 (for a sample with $n = 50$, $t = 1$ nm, this is about two order of magnitude higher than the observed value. It is therefore clear that thicker dielectric layers are required to arrive at the observed value. Such insulating layers are expected to be present in the form of depletion

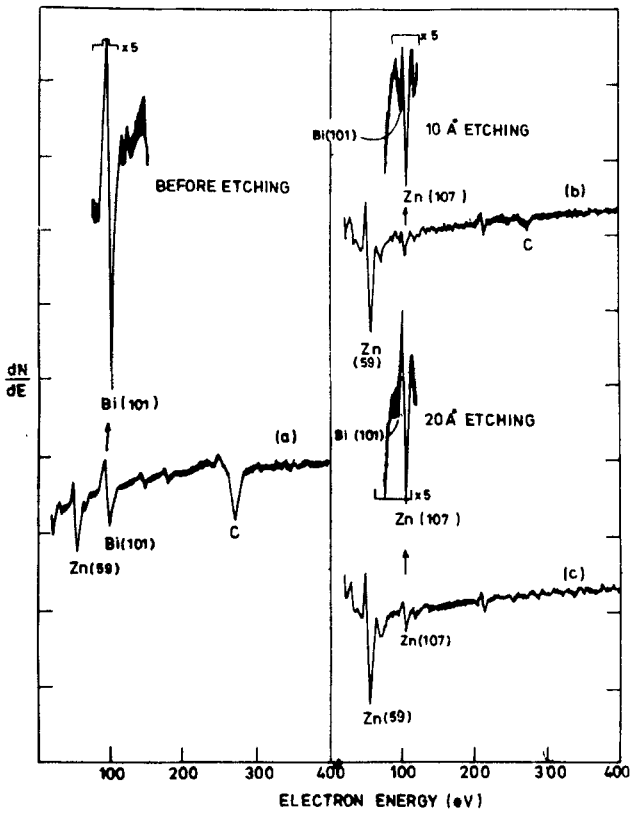

Figure 2. Auger electron spectra of ZnO-Bi_2O_3 (2 wt.%) cersem taken at different depths with sequential ion etching: **a.** Before etching. **b.** 10 Å etching and **c.** 20 Å etching.

layers in the conducting ZnO grains originating at grain intergranular interfaces due to trapping of charge carriers by the surface states/traps and defects present at/near the interface.

In the present case, where two junctions are placed back to back with each other, the total capacitance can be written as

$$(1/C - 1/2\,C_0)^2 = 2(\phi_0 + V)/E\varepsilon_0\varepsilon n_0, \tag{1}$$

where

$$C = e\varepsilon_0\varepsilon n_0/2(\phi_0 \pm V)^{1/2},$$

and

$$\tfrac{1}{2}C_0 = (2\phi_0/e\varepsilon_0\varepsilon n_0), \tag{2}$$

Here C represents the capacitance/junction, n_0, the carrier concentration and ϕ_0, the barrier height.

The width of depletion layer (X_0) and interface charge density (Q) can be estimated using the following standard relations

$$x_0 = (2\varepsilon_0\varepsilon\phi_0/en_0)^{\frac{1}{2}}, \tag{3}$$

$$Q = 2eX_0 n_0. \tag{4}$$

As expected from (1), the plot of $(1/C - 1/2C_0)^2$ vs V of a ZnO-Bi_2O_3, M cersem, shown in figure 3, is a straight line which confirms the barrier model. The values of n_0 and ϕ_0 calculated from the slope and intercept on the voltage axis, respectively, are found to be $2{\cdot}26 \times 10^{18}\,\mathrm{cm}^{-3}$ and 0·85 eV. The density of states N_s at the interface between the ZnO grain and the intergranular layer as estimated from $N_s = (2N_d\varepsilon_s\varepsilon_0\phi_0/q)^{\frac{1}{2}}$ is found to be $4{\cdot}61 \times 10^{12}\,\mathrm{cm}^{-2}$. Nearly the same value of n was

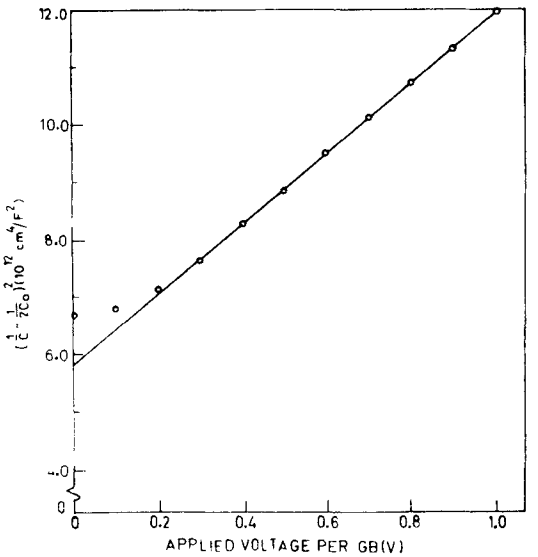

Figure 3. Variation of $\left(\frac{1}{C} - \frac{1}{2C_0}\right)^2$ vs applied voltage per grain boundary of a ZnO multicomponent cersem.

found from the Hall measurements. Also the depletion layer width and capacitance/junction/cm^2 have been calculated to be 60 nm and about 0·15 μF respectively. The latter agrees well with the observed values given in table 1.

Figure 4 shows the variation of dielectric constant of ZnO-Bi_2O_3, M with sintering temperature. It is clear from table 1 and figure 4 that the dielectric constant of the composite increases monotonically with sintering temperature. The observed increase in grain size with sintering temperature (figure 4) helps in explaining the variation of dielectric constant. Higher sintering temperature increases the grain size i.e. lowers n and hence nt resulting in higher values of observed capacitance/cm^2 and dielectric constant. Experimentally observed values of 0·2 to 0·3 μF/cm^2/junction for capacitance agree well with the calculated values. The low values of dielectric constant for linear cersems like ZnO-CoO, ZnO-Cr_2O_3 and ZnO-Bi_2O_3, M sintered at 800°C are understandable because in these systems of microstructurally randomly dispersed constituents there are no segregated intergranular layers between conducting ZnO grains and depletion layers in ZnO grains.

3.2 *Dielectric dispersion at room temperature*

The frequency dependence of the capacitance, the dielectric constant (ε') and tan δ ($=\varepsilon''/\varepsilon'$), where complex dielectric constant $\varepsilon=\varepsilon-j\varepsilon''$, has been carried out for nonlinear cersems of various compositions.

The frequency dependence of capacitance and dielectric constant for a binary ZnO-Bi_2O_3 cersem having a low value ($\sim$6) of nonlinearity parameter is plotted in figure 5. In this case capacitance shows a dispersion in the entire frequency range with its value decreasing with frequency. Similar variation is exhibited by tan δ up to a frequency of 10^4 Hz.

A dissipation maxima (tan δ_{max}) is evident at a frequency of 3×10^5 Hz. The variation of ε' and tan δ as a function of frequency for a ZnO-Bi_2O_3, M cersem is plotted in figure 6. The value of ε' decreases slowly with increasing frequency up to

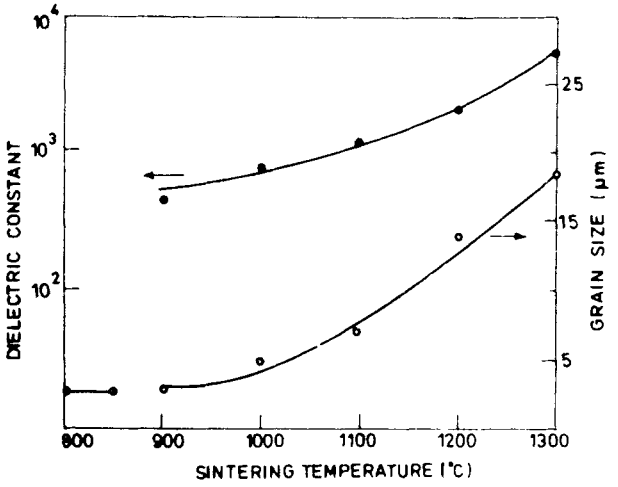

Figure 4. Variation of dielectric constant and grain size with sintering temperature of a ZnO multicomponent cersem.

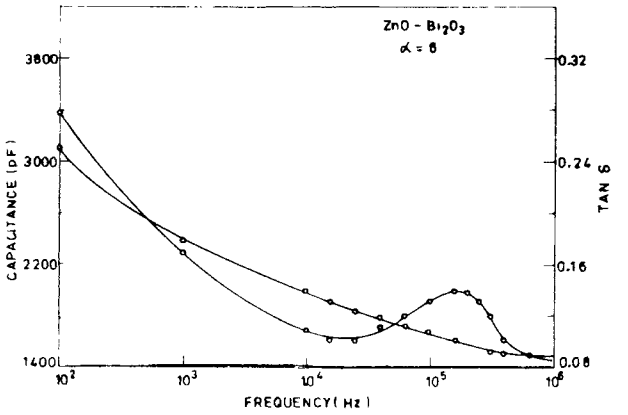

Figure 5. Variation of capacitance and tan δ of a binary cersem with frequency.

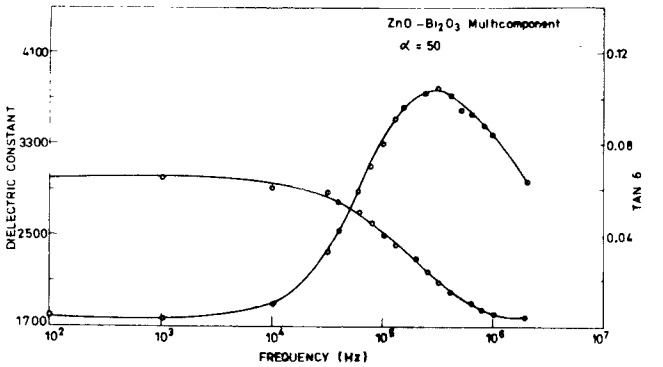

Figure 6. Frequency dependence of dielectric constant (ε') and tan δ of the multicomponent cersem.

about 10^5 Hz and exhibits a noticeably sharper drop in the frequency range 10^5–10^6 Hz. The value of tan δ is very small at low frequencies and does not vary significantly up to a frequency of about 10^4 Hz. Beyond this frequency tan δ increases rapidly and exhibits a maxima around 3×10^5 Hz at room temperature.

It is noteworthy that while the value of capacitance, dielectric constant (ε') and tan δ at low frequencies is dependent on composition and fabrication process, $\tan \delta_{max}$ remains practically unaltered (observed at 3×10^5 Hz) with changes in composition and sintering parameters (Bhushan *et al* 1981). Even in degraded ZnO-Bi_2O_3, M ceramics, Eda (1984) reported the peaking of tan δ at the same frequency of 300 kHz.

Dielectric dispersion can be explained on the basis of Debye-type relaxation by drawing Cole-Cole plot (plot of ε' vs ε'') exhibiting a single or multiple relaxation times. In the present case a Cole-Cole plot for a high nonlinearity cersem is shown in figure 7. It is observed that the experimental data lie on a circular arc centred at a point below the ε'' axis. This suggests a distribution of relaxation times. The value of $n(n = 2\theta/\pi)$ has been found to be about 0·2 which corresponds to a distribution of relaxation time extending over one or two orders of magnitude. Such a Debye-type of relaxation may be attributed to an orientational polarization (Daniel 1967),

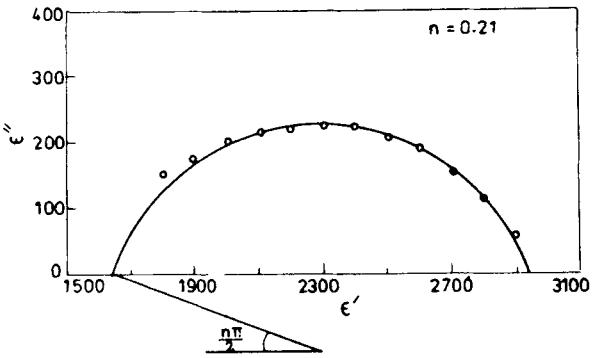

Figure 7. Cole-cole plot for ε' and ε'' of the multicomponent cersem of figure 6.

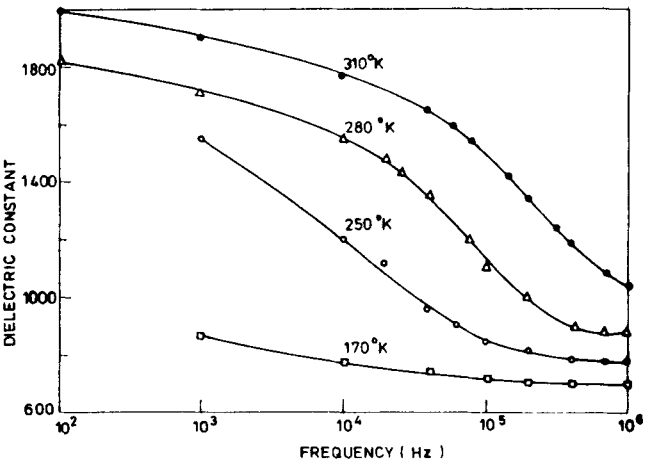

Figure 8. Frequency dependence of dielectric constant of the multicomponent cersem measured at different temperatures.

interfacial polarization (Maxwell-Wagner Model) (Volger 1960) or an electronic phenomena such as hopping, trapping and detrapping of carriers (Jonscher 1981).

In the case of ZnO nonlinear cersems, as shown in figures 5 and 6, the peak position of $\tan\delta$ is independent of composition, and the dielectric constant increases monotonically with temperature (figure 8). Furthermore, these observations cannot be accounted for by orientational polarization because this type of polarization is composition-dependent and the dielectric constant of a material in this case is known to be inversely proportional to temperature (Meakins 1961).

According to interfacial polarization theory, often applied to polycrystalline semiconductors having regions (d_i), of different electrical conductivity (σ_i), and dielectric constant (ε_i), the values of dielectric constants ε_∞ (at $w=\infty$) and ε_s (at $w=0$), are expressed as

$$\varepsilon_\infty = \sum d_i \Big/ \sum (d_i/\varepsilon_i), \tag{5}$$

$$\varepsilon_s = \frac{\left\{\sum d_i\right\}\left\{\sum (d_i \varepsilon_i/\sigma_i^2)\right\}}{\left\{\sum (d_i/\sigma_i)^2\right\}} \tag{6}$$

In the present case the composite is simply assumed to be a mixture of two materials—ZnO grains and depletion regions including intergranular layers. As already established, the depletion layer d_1, is very thin as compared to ZnO grain d_2. Assuming that the intrinsic dielectric constant of the thin layer (most of it extending into ZnO as a depletion layer) has the same value as in the grain ε_2, the expression for ε_∞ reduces to $\varepsilon_\infty = \varepsilon_z = 10$. Since the resistance of the blocking layer has a high value ($d_1\rho_1 \gg d_2\rho_2$), the expression for ε_s reduces to $\varepsilon_s = (d_2/d_1)\varepsilon_2 = 10 \times 10^{-5}$ m/10^{-7} m = 1000, which is nearly half the observed value (figure 6). In this case the loss-factor peaking at frequency ω is expressed as

$$\tan\delta = (d_2/d_1)[\omega\tau_\delta/(1+\omega^2\tau_\delta^2)], \tag{7}$$

where τ_δ, the relaxation time at loss angle, δ, is written as

$$\tau_\delta = (\varepsilon_\infty/\varepsilon_s)^{\frac{1}{2}}\,\varepsilon_0 \frac{\varepsilon_2 d_2 + \varepsilon_2 d_1}{\sigma_2 d_2 + \sigma_2 d_2} \tag{8}$$

Using $\sigma_1 = 10^{-10}$ mho cm^{-1}, $\sigma_2 = 1$ mho cm^{-1}, $\varepsilon_0 = 8{\cdot}845 \times 10^{-12}$ F m^{-1}, and $\tan\delta_{max} = 0{\cdot}14$, the value of f_{max} ($\omega_{max}/2$) is calculated to be nearly 10^{10} Hz, a value which is five orders of magnitude higher than the one obtained experimentally. It is, therefore, concluded that the Maxwell-Wagner theory of interfacial polarization cannot satisfactorily explain the observed dielectric behaviour.

The dielectric loss ($\tan\delta$) vs frequency plots at different temperatures is shown in figure 9. The peak position shifts towards lower frequency with decrease in the temperature of measurement. The above data have been replotted as f_{max} (the frequency at which $\tan\delta_{max}$ occurs) vs $1/T$ in figure 10. An activation energy of

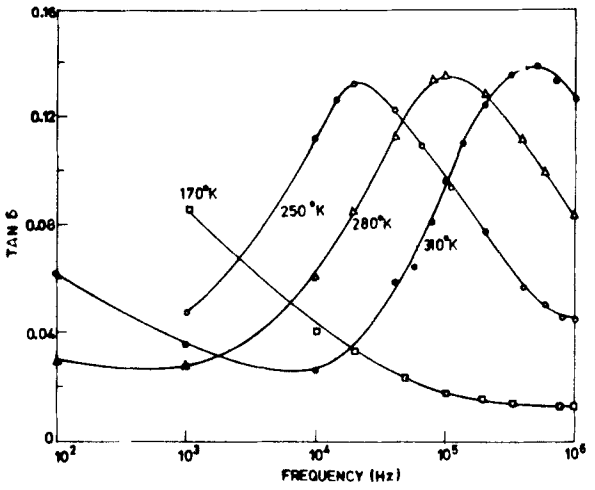

Figure 9. Variation of $\tan\delta$ with frequency of a ZnO multicomponent cersem measured at different temperatures.

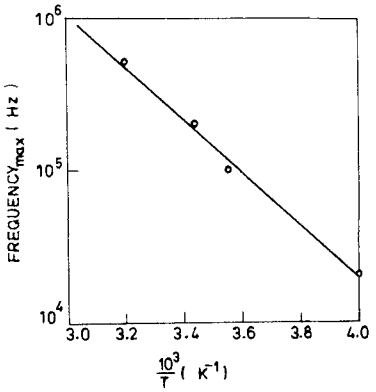

Figure 10. Variation of dissipation factor peak frequency (f_{max}) with inverse temperature of the multicomponent cersem.

0·36 eV, a value in agreement with the one due to Levinson and Philipp (1976), has been estimated from this curve for the dielectric relaxation process giving rise to loss peak.

The observed thermally-activated dissipation peak can be attributed to trapping/detrapping of carriers in the interface states. In the case of insulators and amorphous semiconductors exhibiting a broad distribution of relaxation times (as indeed observed in the present case) the dielectric loss is attributed to the hopping of electrons between localized defect states (Elliot 1984). A similar behaviour observed in *p-n* junction has also been explained on the basis of trapping/detrapping model by Barsony and Jonscher (1978).

It is therefore established that the observed dielectric dispersion of ZnO cersems is caused due to hopping, trapping and detrapping of electrons in the energy states lying in intergranular/depletion layers.

3.3 *Temperature dependence of dielectric constant/capacitance*

It is known that the energy difference between the bottom of the conduction band and the Fermi level E_F is proportional to $[\ln (N_C/N_D)T]$, where N_C is the effective density of states and N_D the donor density. As such, in ZnO with a high donor density, Fermi level is not expected to change significantly with increase in temperature from 100 to 300 K. This in turn will leave the barrier height (ϕ_0) unchanged in this temperature range. The carrier concentration n, as evident from (9) increases with the temperature

$$n=(2N_D)^{\frac{1}{2}}\left(\frac{2\pi m^* kT}{h^2}\right)^{\frac{3}{4}}\exp(-E_d/2KT) \tag{9}$$

where E_d is the ionization energy of donors. The invariance of ϕ_0 and increase of n with change in temperature from 100 to 300 K has been observed by the present authors. It can therefore be inferred from (3) that the thickness of a depletion layer which is inversely proportional to the square root of carrier concentration, decreases with increase in temperature and results in the increase of dielectric constant/capacitance as indeed observed (figures 8 and 11).

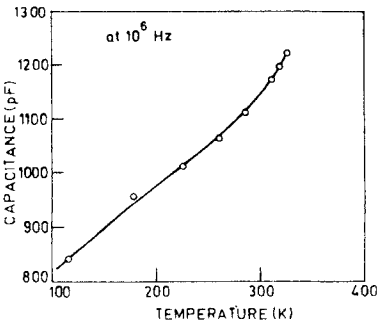

Figure 11. Variation of capacitance with measurement temperature of a ZnO multicomponent cersem.

4. Conclusions

(i) Zinc oxide-based nonlinear cersems exhibit extremely high dielectric constant (upto nearly 3×10^3) as compared to the linear cersems and the individual constituents (up to 30). Such a high dielectric constant arises solely because of a two-phase microstructure.

(ii) The observed high value of dielectric constant has been explained on the basis of depletion layers existing at grain-intergranular interfaces and extending into ZnO grains. Typical thickness of a depletion layer has been estimated to be approximately 10^2 nm. The thickness of an intergranular layer using Auger electron spectroscopy, however, has been determined to be 1 to 2 nm only.

(iii) The dielectric constant of the cersems has been found to depend on the grain-size of conducting ZnO (which in turn is a function of sintering temperature). Increase in sintering temperature results in the increase of both the grain-size and the dielectric constant. The increase in dielectric constant has been successfully explained on the basis of the depletion layer model and the simplified microstructure of the cersems.

(iv) The dielectric constant (ε') and dielectric loss ($\tan\delta$) exhibit a dispersion in the frequency range of 10^2 to 10^6 Hz. While the values of ε' and $\tan\delta$ are quite sensitive to fabrication process at low frequencies, the $\tan\delta$ peak position remains practically unaltered with change in composition or sintering parameters. The dispersion associated with a distribution of relaxation times is explained on the basis of Debye-type relaxation process caused due to trapping/detrapping of electrons in the states available in depletion layer and interface.

(v) The monotonic increase in dielectric constant/capacitance with temperature, in the range of 170 to 310 K, has been attributed to the change in width of the depletion layer brought about by the change in carrier concentration.

Acknowledgement

One of the authors (BB) wishes to acknowledge the financial support from the Indian Institute of Technology, Delhi.

References

Barsony I and Jonscher A K 1978 *Solid State Electron* **21** 471
Bhushan B, Kashyap S C and Chopra K L 1981 *Appl. Phys. Lett.* **38** 160
Bhushan B, Kashyap S C and Chopra K L 1981 *J. Appl. Phys.* **53** 2932
Chopra K L, Bhushan B and Kashyap S C 1983 *J. Appl. Phys.* **54** 1610
Clarke D R 1978 *J. Appl. Phys.* **49** 2407
Daniel V V 1967 *Dielectric relaxation* (New York: Academic Press)
Delaney R A and Kaiser H D 1967 *J. Electrochem. Soc.* **114** 833
Eda K 1984 *J. Appl. Phys.* **56** 2948
Eda K, Iga A and Matsuoka M 1980 *J. Appl. Phys.* **51** 2678
Eda K, Eguchi H, Okinaka H and Matsuoka M 1983 *Jpn. J. Appl. Phys.* **22** 202
Elliot S R 1984 *Physics of amorphous materials* (London: Longman)
Jonscher A K 1981 *6th Progress Report of Chelsea Dielectric Group* (London: University Press)
Levinson L M and Philipp H R 1975 *J. Appl. Phys.* **46** 1332
Levinson L M and Philipp H R 1976 *J. Appl. Phys.* **47** 1117 and 3116
Levinson L M and Philipp H R 1978 *J. Appl. Phys.* **49** 6142
Matsuoka M 1971 *Jpn. J. Appl. Phys.* **10** 736
Matsuura M and Yamaoki H 1977 *Jpn. J. Appl. Phys.* **16** 1261
Meakins R J 1961 *Progress in dielectrics* (London: Heywood) vol. 3
Morris W G 1976 *J. Vac. Sci. Technol.* **13** 926
Mukae K, Tsude K and Nagasawa I 1977 *Jpn. J. Appl. Phys.* **16** 1361
Santhanam A T, Gupta T K and Carlson W G 1979 *J. Appl. Phys.* **50** 852
Volger J 1960 *Progress in semiconductors* (ed.) A F Gibson (New York: John Wiley) vol. 4